European Review for Medical and Pharmacological Sciences 2020; 24: 1186-1194

# Effect of miR-26a-5p on gastric cancer cell proliferation, migration and invasion by targeting COL10A1

H.-H. LI[1], J.-D. WANG[2], W. WANG[1], H.-F. WANG[1], J.-Q. LV[1]

[1]Department of Gastrointestinal Surgery, Shaoxing People's Hospital, Shaoxing Hospital of Zhejiang University, Shaoxing, China
[2]Department of Endoscopy Center, Shaoxing People's Hospital, Shaoxing Hospital of Zhejiang University, Shaoxing, China

*Honghai Li* and *Jindao Wang* contributed equally to this work

**Abstract. – OBJECTIVE: This study explored the effect of miR-26a-5p on cell proliferation, migration, and invasion in gastric cancer by targeting COL10A1.**

**MATERIALS AND METHODS: First, differentially expressed genes were identified from microarray GSE103236 data of human gastric cancer. Then, qRT-PCR was carried out to detect the expression levels of COL10A1 and miR-26a-5p in gastric cancer cells and normal cases. The CCK-8 method was used to test cell proliferation. The colony formation assay was performed for the examination of the cell colony-forming ability, and transwell was applied for the detection of cell migration and invasion. Subsequently, the targeted relationship between miR-26a-5p and COL10A1 was identified by bioinformatics methods and further verified by Dual-Luciferase assay. The rescue experiment was finally conducted to validate the miR-26a-5p-dependent mechanism on cell proliferation, migration, and invasion *via* targeting COL10A1.**

**RESULTS: COL10A1 was found to be highly expressed in gastric cancer cells, while miR-26a-5p was poorly expressed. Silencing COL10A1 inhibited cell proliferation, migration, and invasion in gastric cancer. Besides, miR-26a-5p could function on gastric cancer cells by reducing COL10A1. As well, the rescue experiment suggested that the down-regulation of COL10A1 could reverse the inhibitory effect of miR-26a-5p on gastric cancer cells.**

**CONCLUSIONS: Collectively, miR-26a-5p can potentiate proliferation, migration, and invasion of gastric cancer cells by targeting COL10A1.**

*Key Words:*
MiR-26a-5p, COL10A1, Gastric cancer, Proliferation, Migration and invasion.

### Abbreviations

Gene Expression Omnibus (GEO); the cancer genome atlas (TCGA); glyceraldehyde 3-phosphate dehydrogenase (GAPDH); Roswell Park Memorial Institute-1640 (RPMI-1640); Dulbecco's Modified Eagle's Medium (DMEM); phosphate-buffered saline (PBS); fetal bovine serum (FBS); bicinchoninic acid (BCA); horseradish peroxidase (HRP); real-time quantitative polymerase chain reaction (qRT-PCR); cell counting kit-8 (CCK-8); extracellular matrix (ECM); sodium dodecyl sulfate polyacrylamide gel electrophoresis (SDS-PAGE); albumin from bovine serum (BSA); Tris-Buffered Saline Tween-20 (TBST); enhanced chemiluminescence (ECL); analysis of variance (ANOVA).

## Introduction

Gastric cancer (GC) is one of the most common malignant tumors in the world. Although great progress has been made in recent years, the morbidity of GC still ranks fifth in all malignancies, and mortality ranks third[1]. Despite the reduced morbidity, the high degree of malignancy and early metastasis are two of the reasons leading to poor prognosis[2]. As a long-term progressive disease, GC is associated with the activation of oncogenes or the inactivation of tumor suppressors[3]. Therefore, the identification of new candidate biomarkers can provide insights into the early detection of GC. MicroRNAs (miRNAs) are endogenous non-coding RNAs with a length of approximately 23 nucleotides. They can interact with complementary sequences of the 3'-untranslated region (UTR) within target mRNAs, resulting in the degradation of



*Corresponding Author:* Jieqing Lv, MD; e-mail: DrJieqinglv@163.com

target mRNAs or the inhibition of their translation[4]. Mendell et al[5] have found that miRNAs are involved in almost all known physiological and pathological processes, and some miRNAs have been verified to participate in tumorigenesis and development. MiR-26a has been reported[6-9] to affect the proliferation, metastasis, and apoptosis of GC cells, as well as associate with the diagnosis and prognosis of a variety of tumors. COL10A1, a type of X short-chain collagen belonging to the collagen family, is a principal component of the extracellular matrix, and has been identified to play a key role in several fundamental biological processes, such as cell differentiation, morphogenesis, growth, apoptosis, and migration[10]. Huang et al[11] have observed that high-expression of COL10A1 is correlated with poor prognosis of patients suffering colon cancer. In addition, Li et al[12] revealed that COL10A1 and SOX9 may play key roles in GC progression and have the potential serving as biomarkers and therapeutic targets. However, the role of COL10A1 in the occurrence of GC *via* upstream regulatory genes has not been reported.

In this study, we predicted the targeted relationship between COL10A1 and miR-26a-5p through bioinformatics analysis. The regulatory mechanism of miR-26a-5p in GC was further investigated by various *in vitro* experiments on cell activities, including cell proliferation, migration, and invasion, which could help to find novel strategies on targeted therapy for GC.

## Materials and Methods

### Materials

Human normal gastric epithelial cell GES-1 and human GC cell lines MGC-803, MKN-45, HGC-27, and N87 were purchased from the Cell Resource Center of the Institute of Basic Medical Sciences of the Chinese Academy of Medical Sciences. MiR-26a-5p mimics and inhibitors and their controls were purchased from the Ambion co. (Thermo Fisher Scientific, Waltham, MA, USA). The interference sequence of COL10A1 was designed by the BLOCK-iT™ RNAi Designer website. Dual-Luciferase report assay system was from Promega, Madison, WI, USA. Primary antibodies, COL10A1 and glyceraldehyde 3-phosphate dehydrogenase (GAPDH), and the horseradish peroxidase (HRP)-labeled secondary antibody were from Abcam (Cambridge, UK).

### Bioinformatics Analysis

GC microarray GSE103236 was downloaded from the Gene Expression Omnibus (GEO) database (https://www.ncbi.nlm.nih.gov/geo/), including 9 normal samples and 10 GC samples. Bioconductor-based 'limma' package of R language was utilized to select differentially expressed genes (DEGs) with the empirical Bayes method, and the "annotate" package was employed to annotate these DEGs. Expression profiles of COL10A1 in GC samples were accessed from the tumor database (http://ualcan.path.uab.edu/cgi-bin/ualcan-res.pl) included in The Cancer Genome Atlas (TCGA). Four prediction websites, miRDB, mirDIP, miRWalk, and Targetscan, were used to predict the upstream regulatory miRNAs of COL10A1, respectively. Venn diagram was taken to find the target miRNAs.

### Cell Culture and Transfection

GES-1, HGC-27, and N87 cells were cultured in Roswell Park Memorial Institute-1640 (RPMI-1640; Thermo Fisher Scientific, Waltham, MA, USA) mediums containing 10% fetal bovine serum (Thermo Fisher Scientific, Waltham, MA, USA). MGC-803 cells were grown in Dulbecco's Modified Eagle's Medium (DMEM; Thermo Fisher Scientific, Waltham, MA, USA) medium containing 10% FBS. MKN-45 cells were cultured in RPMI-1640 medium supplemented with 20% FBS. Cells in logarithmic phase were then collected for preparation. qRT-PCR was performed to detect the expression of miR-26a-5p and COL10A1, and cells with significantly higher COL10A1 expression were selected for follow-up experiments. Until the monolayer density reached 50-60%, cells were grouped into si-NC group, si-COL10A1 group, NC mimic group, miR-26a-5p mimic group, NC inhibitor group, miR-26a-5p inhibitor group, NC inhibitor+si-NC group, and miR-26a-5p inhibitor+si-COL10A1 group. MiR-26a-5p mimic, miR-26a-5p inhibitor, si-COL10A1, and their controls were transiently transfected into cells using Lipofectamine® 2000 reagent (Invitrogen, Carlsbad, CA, USA), respectively. Transfected cells were maintained in the corresponding mediums in 5% $CO_2$ at 37° C. After 6 h, the mediums were replaced, and the cells were continuously cultured for 48 h for subsequent experiments.

### Real-Time Quantitative Polymerase Chain Reaction (qRT-PCR)

TRIzol (Thermo Fisher Scientific, Waltham, MA, USA) was used to extract the total RNA from GC cells. Ultraviolet spectrophotometer was employed to determine the RNA concentration. PrimeScript RT kit (TaKaRa, Otsu, Shiga, Japan) was utilized to synthesize the cDNA as a template by reverse transcription reaction. Primers were designed by Primer 5.0 software.

MiR-26a-5p: Forward: 5'-UUCAAGUAAUCCAGGAUAGGCU-3', Reverse: 5'-CCUAUCCUGGAUUACUUGAAUU-3'; COL10A1 Forward: 5'-ATGCTGCCACAAATACCCTTT-3', Reverse: 5'-GGTAGTGGGCCTTTTATGCCT-3'; GAPDH Forward: 5'-GGAGCGAGATCCCTCCAAAAT-3' Reverse: 5'-GGCTGTTGTCATACTTCTCATGG-3'; U6 Forward: 5′- CTCGCTTCGGCAGCACA-3' Reverse: 5′-AACGCTTCACGAATTTGCGT-3'.

qRT-PCR was carried out using the qRT-PCR kit (Fanke Biotechnology, Shanghai, China). The reaction conditions were pre-denaturation at 95°C for 5 min, 30 cycles of 95°C for 40 s, 57°C for 40 s, and 72°C for 40 s, followed by extension at 72°C for 10 min. The relative transcription level of the target RNA = $2^{-\Delta\Delta Ct}$, wherein $DCt=Ct_{(target\ gene)}-Ct_{(internal\ reference\ gene)}$. The expression levels of genes in each group were compared. Each experiment was repeated 3 times and the results were averaged.

### CCK-8 Assay

Cell counting kit-8 (CCK-8; Biolite Biotech, Tianjin, China) was utilized for the detection of cell proliferation. Cells of each group were seeded in 96-well plates at a density of $3 \times 10^4$ cells/well and cultured overnight at 37°C containing 5% $CO_2$. Approximately 10 μL of CCK-8 solution was added per well and then the cells were incubated for 4 h at 37°C. Then, the absorbance value at 450 nm was measured by an ultraviolet spectrophotometer at 0, 24, 48, and 72 h, respectively. The experiment was repeated 3 times.

### Colony Formation Assay

GC cells were firstly digested with trypsin and suspended in the culture solution. Cell suspension (200 cells/dish) was inoculated in culture dishes containing 10 mL of culture solution. After routine culture for 3 weeks, cells were fixed by 4% paraformaldehyde for 15 min, and stained in 0.1% crystal violet for 10 min. Phosphate-buffered saline (PBS) was used to wash off the dye solution. The colony forming rate was calculated as (number of clones / number of cells inoculated) × 100%.

### Cell Migration and Invasion Assays

Migration assay: GC cells in logarithmic growth phase were starved for 24 h and digested and resuspended to a final concentration of $2\times10^5$cells/mL. 0.2 mL of suspension was added to the upper chamber of transwell (Millipore, Billerica, MA, USA), and 700 μL of pre-cooled RPMI-1640 medium containing 20% FBS was added to the lower chamber. Cells were maintained in a culture incubator containing 5% $CO_2$ at 37°C. After 24 h, cells in the upper chamber were wiped off with wet cotton swabs. While cells migrated to the lower chamber were fixed with methanol for 30 min and stained by 0.1% crystal violet for 20 min. Images were captured under an inverted microscope and five fields of view were randomly selected for cell count.

Invasion assay: transwell inserts pre-coated with extracellular matrix (ECM) gel were utilized in this experiment. Cells were starved for 24 h and resuspended in FBS-free RPMI-1640 mediums to a final concentration of $2.5\times10^5$cells/mL. The detailed procedures were conducted similar to the migration assay. The experiment was repeated triplicate.

### Western Blot

After transfection for 48 h, the cells were washed 3 times in cold PBS. Proteins were extracted from cells on ice using the whole cell lysate and quantitated by bicinchoninic acid (BCA) quantification kit (Thermo Fisher Scientific, Waltham, MA, USA). Subsequently, the proteins were separated by sodium dodecyl sulfate polyacrylamide gel electrophoresis (SDS-PAGE) at 100V and transferred onto the NC membrane at 100 mA for 120 min. 5% albumin from bovine serum (BSA)/Tris-Buffered Saline Tween-20 (TBST) was used to block the membrane for 60 min. Thereafter, the membrane was incubated with primary antibodies overnight at 4°C, followed by horseradish peroxidase (HRP)-labeled secondary antibody goat anti-rabbit IgG at room temperature for 120 min. Primary antibodies were COL10A1 (ab34710, 1:1000, Abcam, Cambridge, UK) and glyceraldehyde-3-phosphate dehydrogenase (GAPDH) (ab181602, 1:10000, Abcam, Cambridge, UK). TBST was used to wash the membrane 3 times. Enhanced chemiluminescence detection kit (ECL) was employed

to visualize the protein bands and Quantity One software was utilized for the analysis of the gray-scale value. The relative expression of COL10A1 was detected and expressed by the ratio of the gray-scale value of the target band to the internal reference band. The experiment was repeated 3 times.

### Dual-Luciferase Assay

Cells were digested with trypsin (Gibco, Rockville, MD, USA), centrifuged, and re-suspended in cell culture mediums containing 10% FBS. Sequentially, cells were inoculated in 48-well plates at a density of $4\times10^4$ cells/well for 24 h (cell density of 40%-50%). MiR-26a-5p mimic (20 nmol/L), Luciferase reporter vectors wild-type COL10A1, and mutant COL10A1 (COL10A1-wt and COL10A1-mut, 80 ng), as well as pRL-TK (*Renilla* Luciferase protein as the internal reference, 40 ng) were co-transfected into cancer cells. After 48 h of transfection, multifunctional enzyme marker was used to measure Luciferase activity.

### Statistical Analysis

All data were processed using SPSS 22.0 statistical software (IBM, Armonk, NY, USA). The measurement data were expressed in the form of mean ± standard deviation. The comparison between the two groups was performed by *t*-test. The comparison among multiple groups was analyzed by one-way analysis of variance (ANOVA). Tukey's test was used for post-hoc test. $p<0.05$ was regarded as statistically significant.

## Results

### High Expression of COL10A1 in GC Cells

GEO database was utilized to perform differential analysis on COL10A1 in GC microarray GSE103236. As shown in Figure 1A, COL10A1 was highly expressed in GC tissues. Meanwhile, the expression of COL10A1 in matched clinical samples (Figure 1B) showed the same trend and was correlated with patients prognosis as shown in Figure 1C. qRT-PCR was used to detect the expression of COL10A1 in human normal gastric epithelial cell GES-1 and human GC cell lines MGC-803, MKN-45, HGC-27, and N87. As shown in Figure 1D, the expression of COL10A1 in GC cells was significantly up-regulated relative to that in GES-1 cells ($p<0.05$), especially in MKN-45 cell line ($p<0.01$). Therefore, MKN-45 cell line was selected for subsequent experiments

.

### Inhibition of GC Cell Proliferation by Silencing COL10A1

After transfection with three types of siRNAs, qRT-PCR was employed to detect the interference efficiency of COL10A1. As shown in Figure 2A, COL10A1 in the cells transfected with COL10A1-siRNA1, COL10A1-siRNA2, and COL10A1-siRNA3 was significantly decreased ($p<0.05$), while that with COL10A1-siRNA3 was substantially decreased ($p<0.01$). Thus COL10A1-siRNA3 was selected for interference transfection. As revealed by CCK-8 in Figure 2B, cells in si-COL10A1 group had lower proliferation rate relative to those in si-NC group ($p<0.05$). The colony formation assay was performed, finding that compared with si-NC group, the colony forming ability of MKN-45 cells in si-COL10A1 group was significantly reduced ($p<0.05$).

### Inhibition of Cell Migration and Invasion by Silencing COL10A1

The transwell migration and invasion assays were applied to detect the migration and invasion ability of cells in si-NC group and si-COL10A1 group. As shown in Figure 3, compared with the si-NC group, the number of migrated and invasive cells in the si-COL10A1 group was significantly reduced ($p < 0.05$).

### Targeted Regulation of MiR-26a-5p on COL10A1 In the Upstream

MiRDB, mirDIP, miRWalk, and Targetscan four prediction websites were used to predict the regulatory miRNAs of COL10A1. Venn diagram was drawn for searching the target miRNAs (Figure 4A). As shown in Figure 4B, targeted binding sites of miR-26a-5p on COL10A1 were observed within the 3' UTR. Dual-Luciferase assay was conducted to further verify such targeted relationship, finding that the Luciferase activity in the COL10A1-wt and miR-26a-5p co-transfection group was markedly reduced relative to that in the COL10A1-wt and NC co-transfection group ($p<0.05$). Subsequently, the protein levels of COL10A1 in the NC mimic group and the miR-26a-5p mimic group were tested by Western blot. As shown in Figure 4C, miR-26a-5p mimic significantly reduced the COL10A1 protein level in comparison with NC mimic ($p < 0.05$).

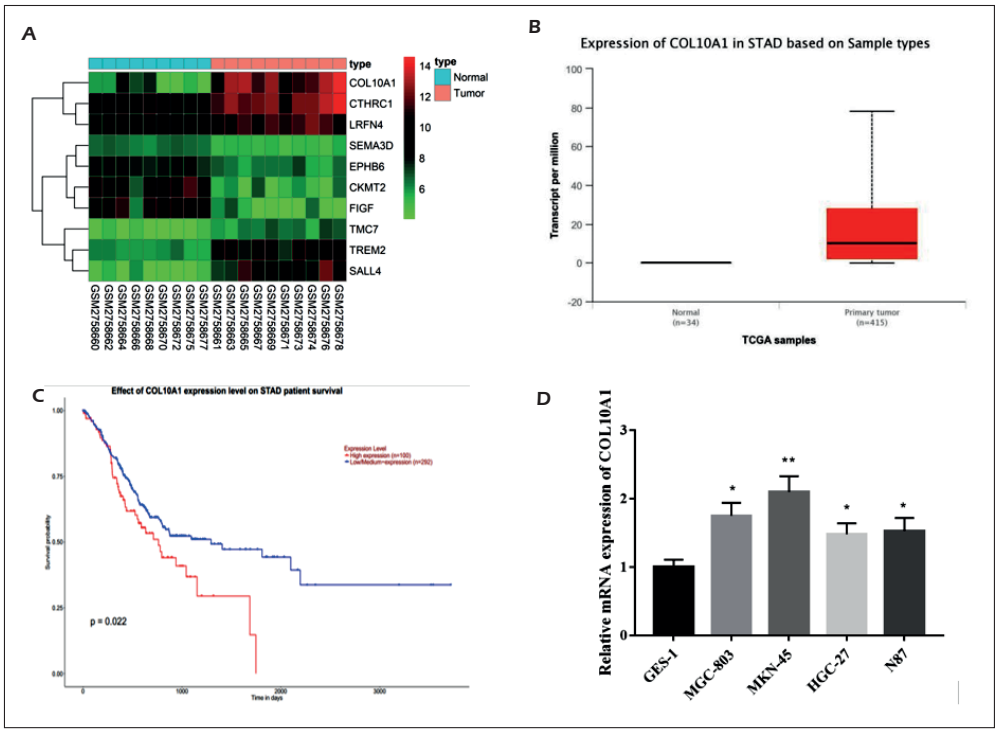


**Figure 1.** High expression of COL10A1 in GC cells. **A**, Thermography of DEGs in GSE103236; **B**, Expression of COL10A1 in TCGA-STAD dataset; **C**, Survival analysis of COL10A1 in TCGA-STAD dataset. Red represents high expression, blue represents low/medium expression; **D**, Expression of COL10A1 in different GC cell lines tested by qRT-PCR ("*" means $p<0.05$, "**" means $p<0.01$).

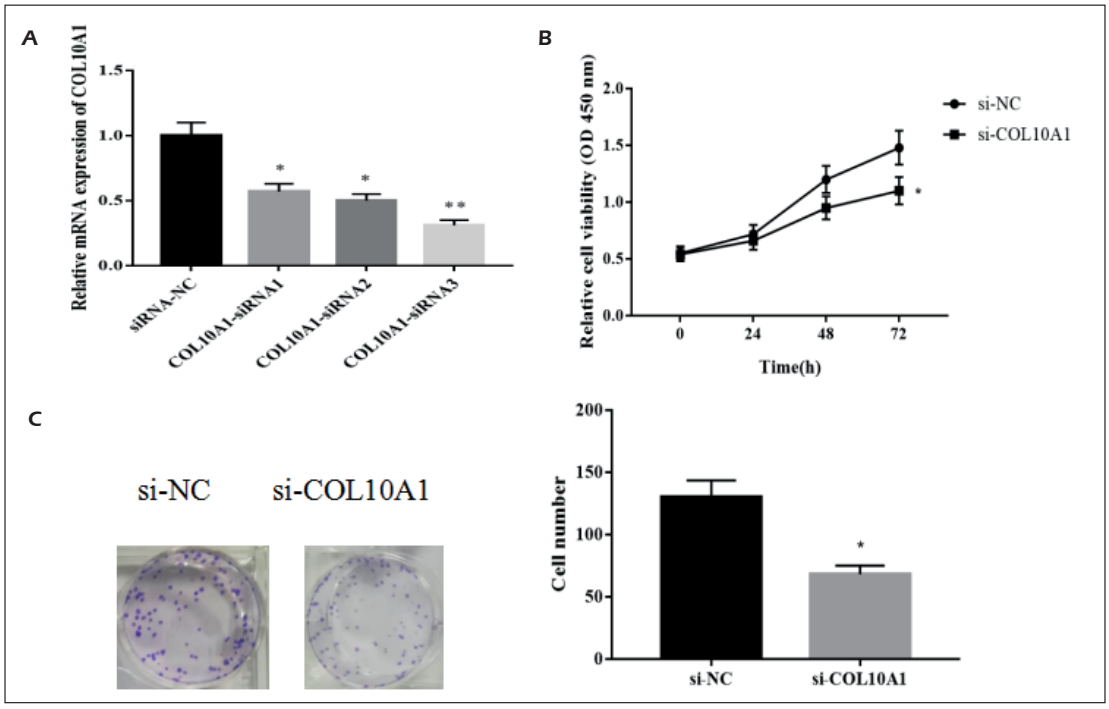


**Figure 2.** Inhibition of COL10A1 Silencing on the proliferation of GC cells. **A**, Interference efficiency of COL10A1 detected by qRT-PCR; **B**, Proliferation rate of cells in si-NC group and si-COL10A1 group examined by CCK-8; **C**, Colony forming ability of cells in si-NC group and si-COL10A1 group measured by colony formation assay ("*" means $p<0.05$, "**" means $p<0.01$).

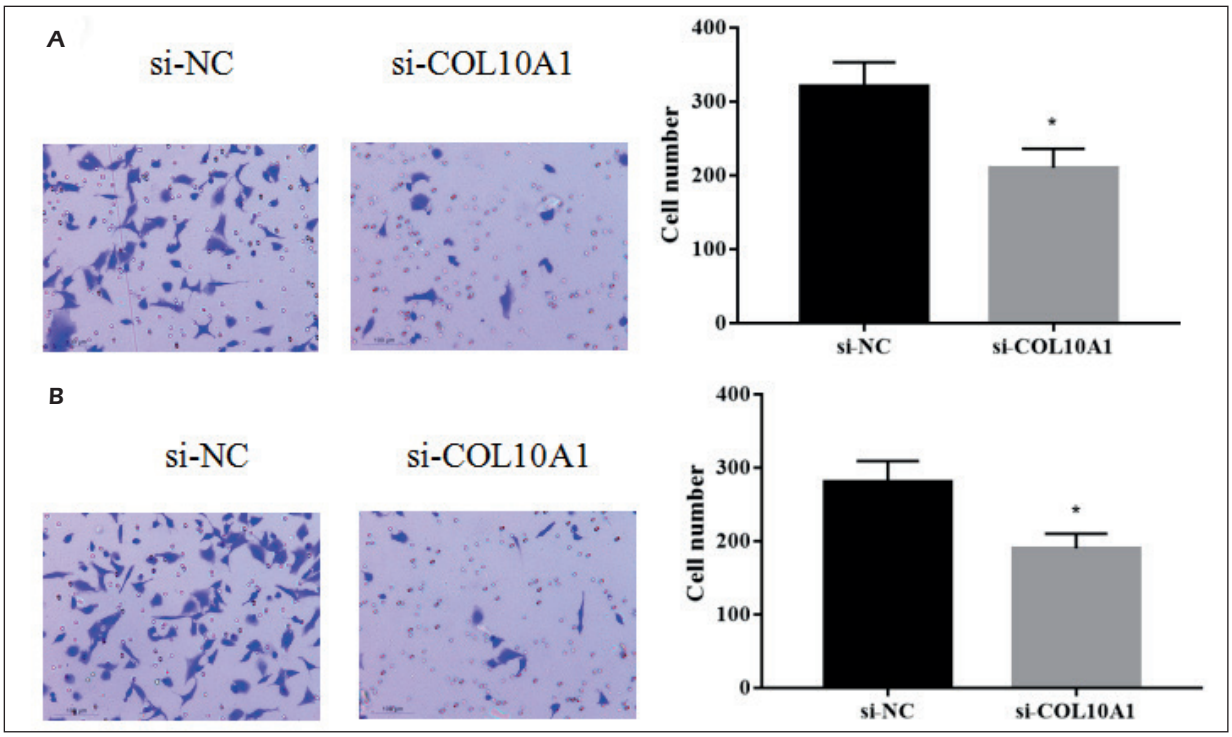


**Figure 3.** Inhibition of COL10A1 Silencing on the migration and invasion of GC cells. **A**, Migration results of each group (magnification: 200X); **B**, Invasion results of each group (magnification: 200X) ("*" means $p<0.05$).

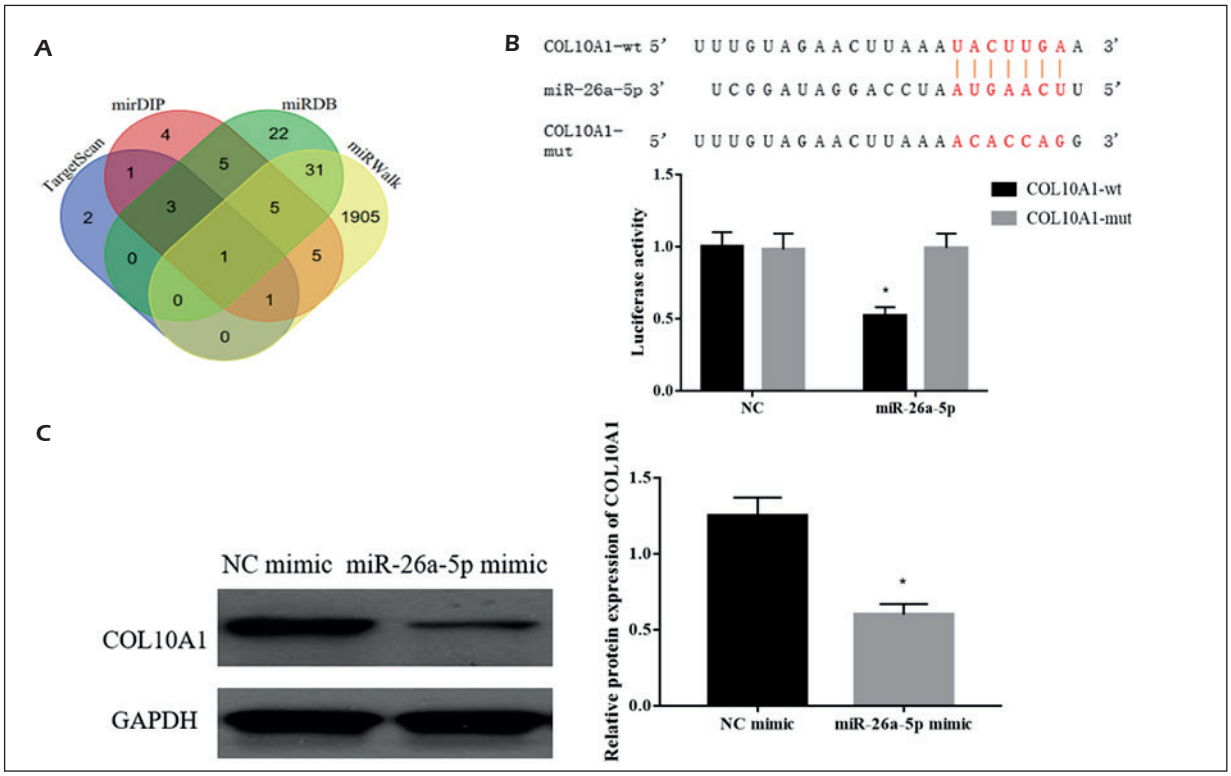


**Figure 4.** Targeted Regulation of miR-26a-5p on COL10A1. **A**, Venn diagram of predicted miRNAs; **B**, Targeted relationship between miR-26a-5p and COL10A1 verified by dual-luciferase assay; **C**, Expression of COL10A1 in NC mimic group and miR-26a-5p mimic group after transfection detected by Western blot ("*" means $p<0.05$).

### *Inhibition of MiR-26a-5p on the Proliferation of GC Cells Through Targeting COL10A1*

qRT-PCR was performed to assess the expression of miR-26a-5p in human normal gastric cell and cancer cell lines. As shown in Figure 5A, miR-26a-5p was markedly reduced in cancer cells by comparison with the normal gastric cells ($p<0.05$). In addition, as revealed by CCK-8 and colony formation assay in Figure 5B, cells treated with miR-26a-5p inhibitor + si-NC had significantly increased proliferation rate and enhanced colony forming ability relative to those with either miR-26a-5p inhibitor+si-COL10A or the negative control ($p<0.05$). Besides, there was no significant difference observed between cells transfected with miR-26a-5p inhibitor+si-COL10A and with the negative control.

### *Inhibition of MiR-26a-5p on the Migration and Invasion of GC Cells Through Targeting COL10A1*

Transwell was performed to assess the migration and invasion ability of cells transfected with NC inhibitor+si-NC, miR-26a-5p inhibitor+si-NC, and miR-26a-5p inhibitor+si-COL10A1. Results showed in Figure 6 suggested the significant increase in the number of migrated and invasive cells in the miR-26a-5p inhibitor+si-NC group relative to that in the NC group ($p<0.05$). When COL10A1 and miR-26a-5p were simultaneously knocked down, the cell number was significantly reduced ($p<0.05$), which was near to the NC group.

## Discussion

GC accounts for the majority of cancer-related deaths in Asian countries. However, cascade events that occur during the onset remain to be fully understood[13]. Increasing evidence[14] has proved that miRNAs might play an important role in the tumorigenesis and development of GC. MiR-383-5p is shown to be down-regulated in GC cells and seen to promote proliferation and migration[15]. Elevated expression of miR-301-3p can accelerate the growth of GC cells[16]. Previous studies have showed that miR-26a-5p can function on the regulation of tumorigenesis and devel-

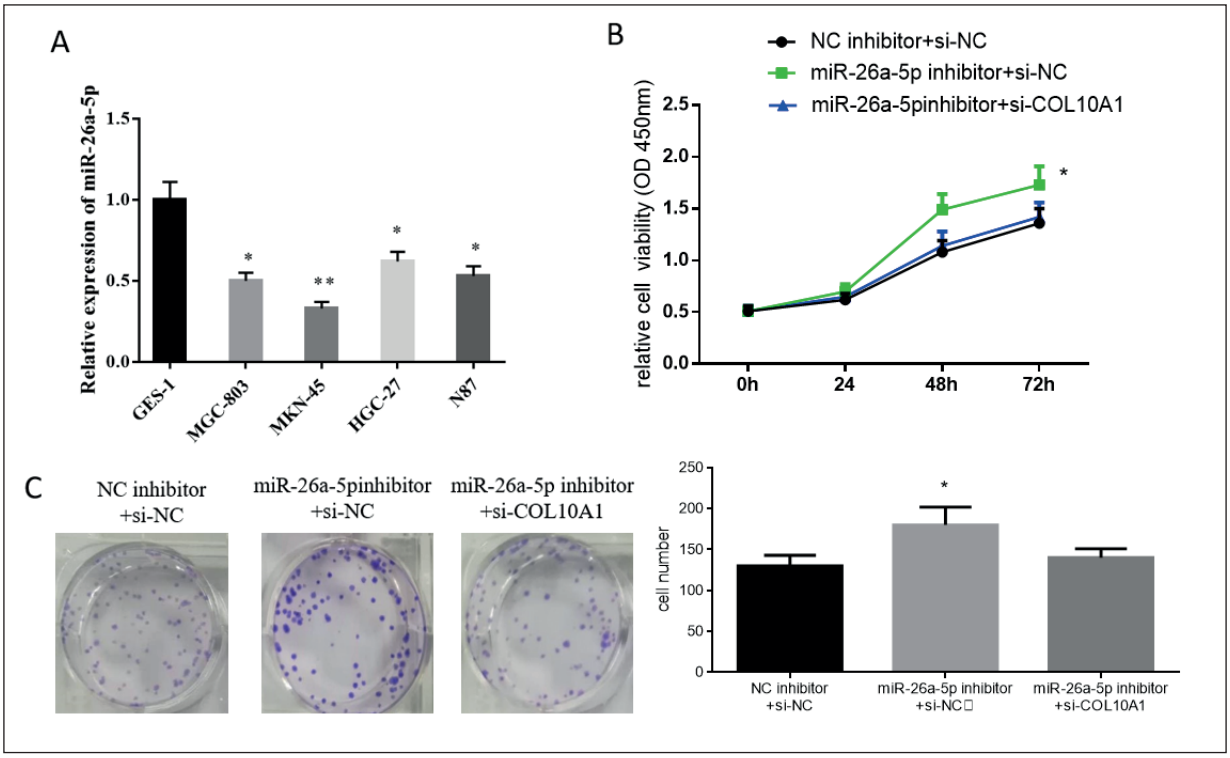


**Figure 5.** Inhibition of miR-26a-5p on the proliferation of GC cells through targeting COL10A1. **A**, Expression of miR-26a-5p in human normal epithelial cells and human GC cell lines assayed by qRT-PCR; **B**, Proliferation rate of cells in each group detected by CCK-8; **C**, Colony forming ability of cells in each group measured by colony formation assay ("*" means $p<0.05$, "**" means $p<0.01$).

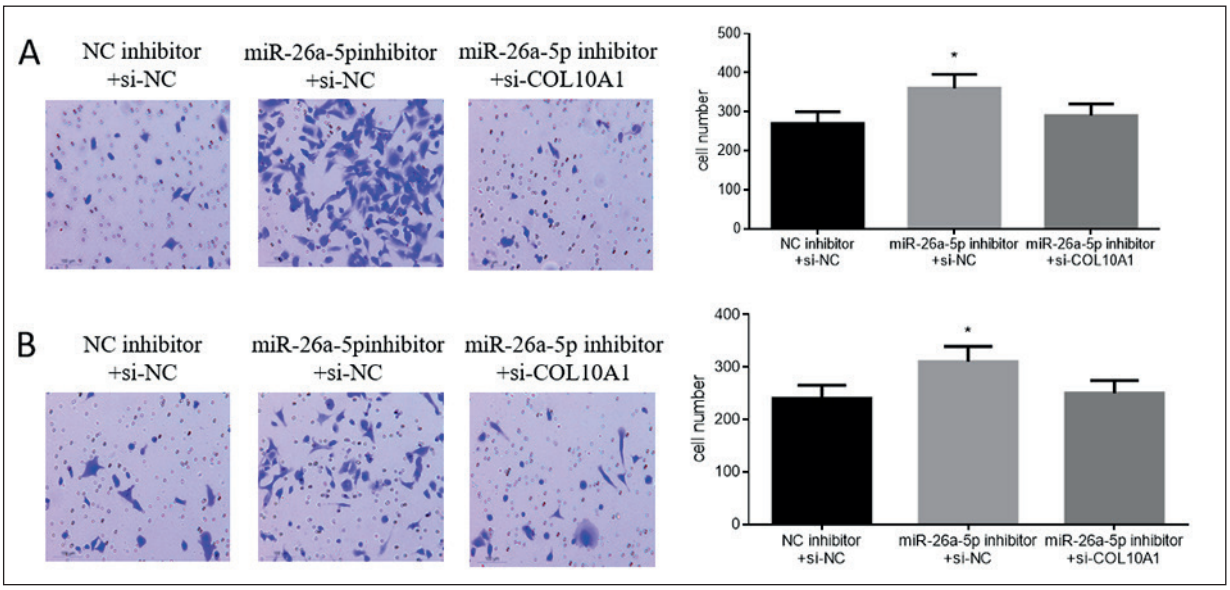


**Figure 6.** Inhibition of miR-26a-5p on the migration and invasion of GC cells through targeting COL10A1. **A**, Migration results of each group cells (magnification: 200×); **B**, Invasion results of each group cells (magnification: 200×) ("*" means $p<0.05$).

opment of GC and has been used as an important biomarker for GC prognosis. MiR-26a can target HGF-VEGF axis consequently suppressing tumorigenesis and angiogenesis[17]. Despite targeted inducing the transcription of conventional oncogenes and inhibiting translation, miR-26a-5p is also involved in the regulation of inflammatory responses, as well as the stemness of stem cells[8,9]. In rheumatoid arthritis rats, miR-26a functions on cartilage injury and chondrocyte proliferation and apoptosis by regulating CTGF[8]. Moreover, miR-26a-5p can participate in the regulation of osteogenic differentiation of human periodontal ligament stem cell from inflammatory microenvironment *via* the interaction with Wnt5a[18]. COL10A1 knockdown is known to associate with the decrease in matrix metalloproteinases (MMP2 and MMP9), as well, it plays an important role in the treatment of invasive tumors metastasis and the control of cancer development[19]. COL10A1 overexpression has been approved to contribute to the promotion of cell migration and invasion in GC, but the mechanism of COL10A1 mediated by miRNAs on GC is still unclear.

## Conclusions

We predicted and verified the upstream miRNA of COL10A1 and found that miR-26a-5p could function on the proliferation, migration, and invasion of GC cells by down-regulating COL10A1. Our results further emphasized that miR-26a-5p is a key tumor suppressor and regulated by epigenetic mechanisms of GC. Suppressing COL10A1 might be a promising approach for better GC treatment.

### Conflict of Interest

The Authors declare that they have no conflict of interests.

## References

1) Bray F, Ferlay J, Soerjomataram I, Siegel RL, Torre LA, Jemal A. Global cancer statistics 2018: GLOBOCAN estimates of incidence and mortality worldwide for 36 cancers in 185 countries. CA Cancer J Clin 2018; 68: 394-424.

2) Veronese N, Fassan M, Wood LD, Stubbs B, Solmi M, Capelli P, Pea A, Nottegar A, Sergi G, Manzato, Carraro S, Maruzzo M, Cataldo I, Bagante F, Barbareschi M, Cheng L, Bencivenga M, De Manzoni G, Luchini C. Extranodal extension of nodal metastases is a poor prognostic indicator in gastric cancer: a systematic review and meta-analysis. J Gastrointest Surg 2016; 20: 1692-1698.

3) Berger H, Marques MS, Zietlow R, Meyer TF, Figueiredo CJH. Gastric cancer pathogenesis. Helicobacter 2016; 21: 34-38.

4) Shukla GC, Singh J, Barik S. MicroRNAs: processing, maturation, target recognition and regulatory functions. Mol Cell Pharmacol 2011; 3: 83-92.

5) Mendell JT, Olson EN. MicroRNAs in stress signaling and human disease. Cell 2012; 148: 1172-1187.

6) Wang CJ, Zhu CC, Xu J, Wang M, Zhao WY, Liu Q, Zhao G, Zhang ZZ. The lncRNA UCA1 promotes proliferation, migration, immune escape and inhibits apoptosis in gastric cancer by sponging anti-tumor miRNAs. Mol Cancer 2019; 18: 115.

7) Ding K, Wu Z, Wang N, Wang X, Wang Y, Qian P, Meng G, Tan S. MiR-26a performs converse roles in proliferation and metastasis of different gastric cancer cells via regulating of PTEN expression. Pathol Res Pract 2017; 213: 467-475.

8) Jiang L, Cao S. Role of microRNA-26a in cartilage injury and chondrocyte proliferation and apoptosis in rheumatoid arthritis rats by regulating expression of CTGF. J Cell Physiol 2019; 235: 979-992.

9) Deng M, Tang HL, Lu XH, Liu MY, Lu XM, Gu YX, Liu JF, He ZM. miR-26a suppresses tumor growth and metastasis by targeting FGF9 in gastric cancer. PLoS One 2013; 8: e72662.

10) Boudreau N, Bissell MJ. Extracellular matrix signaling: integration of form and function in normal and malignant cells. Curr Opin Cell Biol 1998; 10: 640-646.

11) Huang H, Li T, Ye G, Zhao L, Zhang Z, Mo D, Wang Y, Zhang C, Deng H, Li G, Liu H. High expression of COL10A1 is associated with poor prognosis in colorectal cancer. Onco Targets Ther 2018; 11: 1571-1581.

12) Li T, Huang H, Shi G, Zhao L, Li T, Zhang Z, Liu R, Hu Y, Liu H, Yu J, Li G. TGF-beta1-SOX9 axis-inducible COL10A1 promotes invasion and metastasis in gastric cancer via epithelial-to-mesenchymal transition. Cell Death Dis 2018; 9: 849.

13) Zhao X, Yang L, Hu J. Down-regulation of miR-27a might inhibit proliferation and drug resistance of gastric cancer cells. J Exp Clin Cancer Res 2011; 30: 55.

14) Ueda T, Volinia S, Okumura H, Shimizu M, Taccioli C, Rossi S, Alder H, Liu CG, Oue N, Yasui W, Yoshida K, Sasaki H, Nomura S, Seto Y, Kaminishi M, Calin GA, Croce CM. Relation between microRNA expression and progression and prognosis of gastric cancer: a microRNA expression analysis. Lancet Oncol 2010; 11: 136-146.

15) Wei C, Gao JJ. Downregulated miR-383-5p contributes to the proliferation and migration of gastric cancer cells and is associated with poor prognosis. PeerJ 2019; 7: e7882.

16) Fan H, Jin X, Liao C, Qiao L, Zhao W. MicroRNA-301b-3p accelerates the growth of gastric cancer cells by targeting zinc finger and BTB domain containing 4. Pathol Res Pract 2019; 215: 152667.

17) Si Y, Zhang H, Ning T, Bai M, Wang Y, Yang H, Wang X, Li J, Ying G, Ba Y. MiR-26a/b inhibit tumor growth and angiogenesis by targeting the HGF-VEGF axis in gastric carcinoma. Cell Physiol Biochem 2017; 42: 1670-1683.

18) Zhang KK, Geng YD, Wang SB, Huo L. MicroRNA-26a-5p targets Wnt5a to regulate osteogenic differentiation of human periodontal ligament stem cell from inflammatory microenvironment. Zhonghua Kou Qiang Yi Xue Za Zhi 2019; 54: 662-669.

19) Zheng H, Takahashi H, Murai Y, Cui Z, Nomoto K, Niwa H, Tsuneyama K, Takano Y. Expressions of MMP-2, MMP-9 and VEGF are closely linked to growth, invasion, metastasis and angiogenesis of gastric carcinoma. Anticancer Res 2006; 26: 3579-3583.